The Impact of Thermal Degradation on Properties of Electrical Machine Winding Insulation Material

M. Sumislawska, K. N. Gyftakis, *Member IEEE*, D. F. Kavanagh, M. McCulloch, *Senior Member IEEE*, K. J. Burnham, and D. A. Howey, *Member IEEE*

***Abstract* — Inter-turn stator short circuits can develop quickly leading to serious damage of an electric machine. However, degradation mechanisms of winding insulation material are not yet fully understood. Therefore, the main contribution of this article is analysis of the impact of thermal ageing on the electrical properties of the thin film winding insulation. The insulation samples have been aged thermally at 200–275 °C and for 100–1600 hours. After ageing, impedance spectroscopy measurements were undertaken on the samples and equivalent circuit model (ECM) parameters fitted for each measurement. This allows the impact of thermal ageing on ECM parameters to be analysed, giving insight into the changes of the electrical properties of the insulation. Finally, high voltage was applied to the samples aiming to identify the breakdown voltage characteristics of the insulation material.**

Index Terms* — *equivalent circuit model, electric machine, impedance spectroscopy, polyamide-imide, stator winding, thermal degradation

I. Introduction

STATOR faults are an important cause of electrical machine failures. The appearance of stator faults depends on the size of the electrical machine. According to [1], low voltage induction motor stator faults account for only 9% of total failures. In medium voltage induction motors, the percentage increases to 35-40%, whereas for high voltage it is more than 65% [2]-[6]. Amongst all possible stator faults, inter-turn stator faults are of particular interest because they are challenging to detect, especially at low severity levels [7]-[10], however they can evolve quickly leading to serious motor damage [11]. Moreover, these faults are difficult to discriminate from stator voltage supply imbalances. As a consequence, a variety of fault detection techniques including neural networks and envelope analysis have recently been applied [12]-[17].

Alternatively, other researchers have tried to understand directly the physical mechanisms that lead to insulation degradation [18], leading to lifetime prediction and machine life prognosis models that may be used to improve performance and reduce cost. It is now well known that there are many different ageing stresses: electrical, thermal, mechanical, humidity, moisture etc [19]. There have been many studies aimed at understanding insulation thermal ageing. An effort is made here to review and summarise some important past contributions.

Firstly, it has been noted that on-line thermal and chemical monitoring techniques are cost effective only in large machines [20]. Moreover, protective relays are triggered after the insulation has been seriously damaged and thus they cannot be considered to help towards the monitoring of the fault especially at low severity levels [21].

Furthermore, there are a variety of techniques which deal with the ageing mechanisms of the electrical machine windings insulation. In [22] a significant resin weight loss was observed around the winding in a failed induction motor. Additionally, it was found in [23] that after the initial ageing cycles, there was a shift of the dissipation factor and the capacitance at all voltage levels towards lower losses and capacitances because of the drying out and post curing of the insulation. Moreover, a new life span model was developed in [24], which presents an original relationship between the insulation life span and the stress parameters with the application of the Design of Experiments (DoE) methodology. Also, in [25] a new cable monitoring method was proposed based on impedance spectrum analysis in the high frequency range. Furthermore, in [26] the authors used a regression tree constructed with 32 experiments for insulation lifespan modelling (twisted pairs). One of their findings is that at low voltages, only the temperature has a significant effect on the lifespan. In the same work, in parametric Design of Experiments (DoE) and Response Surface (RS) models, the lifespan is expressed as a linear additive function of the predictors and their effects. The most influent factors and interactions were identified as those having the highest estimated effects: the voltage V, the temperature T, their interaction, and the T^2. Finally, in [27] the authors experienced a 20% capacitance drop of their tested windings after 5 thermal cycles. In the same work, they proposed a method, which is based on the monitoring of the current transients after step voltage excitation applied by the inverter and was applied on a high voltage induction motor.

In the above papers the most commonly applied degradation technique is that of accelerated ageing, which deserves some further explanation. It has been reported in [25] that unstrained tests give overly optimistic information relating to long-term design data or predictions of expected lifetime. Furthermore, this type of testing has limitations. If the applied temperature exceeds some critical value then different chemical reactions are caused compared to the real

ageing mechanisms. However, in [26] the application of multi-stress ageing on stator bars was successful in predicting the real ageing mechanisms of actual bars in applications working for 22 years. In the same work, the significant role of mechanical stress is highlighted because the loosening of the stator bars in the slots leads to vertical vibrations which enhance the degradation mechanism.

Most of the research in the topic of electric machine insulation degradation focuses on the behaviour of the whole winding or twisted pair samples. Due to the nature of such research the insulation is subjected to multiple types of stress at once (thermal, mechanical, etc.). However, not much attention has been paid to the properties of the insulation material itself. Therefore, in this article we investigate properties of thin film insulation material subjected to an isolated thermal stress. Thus, the research presented in this paper supplements the work on more complex geometries, such as the twisted pairs and the windings.

The results presented in this paper are part of an ongoing study of the impact of thermal degradation on the properties of thin film insulation material. The work presented in this article is a continuation of our research described in [31]. The main contributions of this article are the following: Section III provides estimation accuracy for resistance and capacitance measurements. In Section IV the dielectric measurements of new (unaged) samples are analysed in order to verify the consistency of dielectric properties of new samples (this allows to determine manufacturing quality of new insulation samples and forms a baseline for degradation analysis). In Section V the variations of insulation dielectric properties as for different temperatures are analysed to a greater extent than in [31]. Finally, the breakdown voltage characteristics of the tested samples after the application of high voltage stress are illustrated in Section VI leading to a development of a breakdown voltage model as function of temperature.

II. Experiment design

Sample specimens were prepared from industrial grade class H, polyester 200 rectangular enamel wire (IEC 60317-29 standard). The rectangular wire (15.5 mm × 2.5 mm) was cut into specimens that were 350 mm long. Both ends of the specimens were drilled for making electrical connection points for dielectric measurement purposes. One hundred and eighty of these polyamide-imide (PAI) insulation samples were then divided into six groups of thirty samples each. Each group of samples were placed into separate laboratory thermal chambers. These chambers were set to temperature set points of 200, 215, 230, 245, 260, and 275 °C, respectively. Each group of samples that were aged at the same temperature was further divided into 5 subgroups of 6 samples each. Each subgroup was aged for a different period of time at a fixed temperature, these ageing time durations were 100, 200, 400, 800, and 1600 hours, respectively. After the thermal ageing, samples were placed in specially fabricated plastic holders and the impedance responses were measured at six equally spaced points 40 mm apart along the sample specimens using a dielectric probe test fixture (the parallel plate method [28]). The impedance measurement equipment used was the N4L PSM1735 Impedance Analyzer using a dielectric probe based on the standard ASTM D150 - 11. The impedance measurements (C, DF, $|Z|$ and Θ) were made over the frequency range 1 Hz to 20 MHz.

Furthermore, impedance spectroscopy of twenty new (i.e. unaged) insulation samples was carried out in the same manner for comparison with the aged samples. Further details of the experiment design can be found in [31].

III. Equivalent circuit model

Impedance spectroscopy of an example insulation sample is presented in Fig. 1. The insulation exhibits capacitive behaviour for frequencies above 1 kHz, whilst for frequencies below 1 kHz the impedance is mainly resistive.

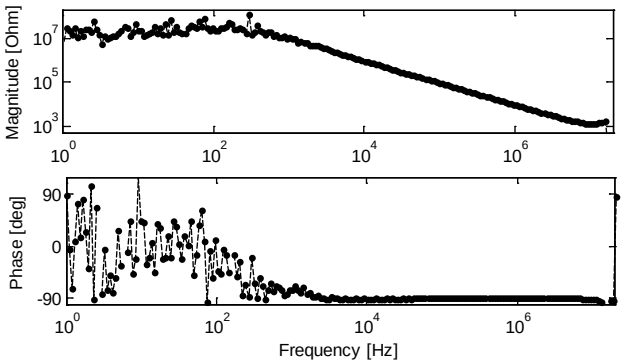

Fig. 1. Impedance spectroscopy of insulation sample

The insulation impedance response has been modelled using an equivalent circuit model comprising a capacitor C and resistor R connected in parallel

$$Z(j\omega) = \frac{R}{RCj\omega+1} \quad (1)$$

where ω is the frequency expressed in radians per second and $j = \sqrt{-1}$. The R and C parameters of the equivalent circuit model have been fitted and histograms of parameters of new samples are plotted in Fig. 2. Estimation uncertainties (assuming 95 % confidence bounds, see [32] for more details) of R and C are analyzed in the following subsections.

A. Uncertainty of resistance estimation

Fig. 3 presents the uncertainty of the resistance estimation, denoted δR, vs. the fitted value of resistance for all measurements of the unaged samples. It is observed that the resistance estimation uncertainty is proportional to the value

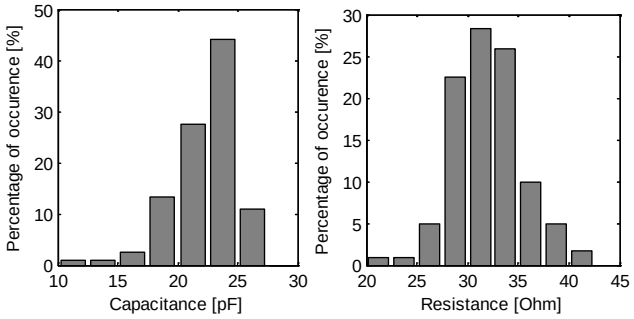

Fig. 2. Histograms of capacitance and resistance of unaged insulation

of resistance R and has been obtained with $\delta R/R \cong 19\%$ accuracy on average. A similar observation has been made with respect to the aged insulation samples. This relatively high uncertainty is due to significant levels of measurement noise observed at low frequencies (where behaviour of the insulation is resistive, see Fig. 1) caused by the inability of the measurement equipment to drive the extremely small currents required for the measurements in this range.

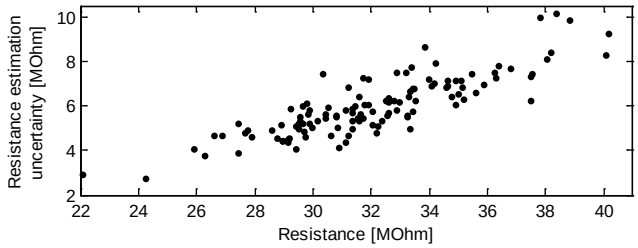

Fig. 3. Uncertainty of resistance estimation vs. resistance estimate

B. *Uncertainty of capacitance estimation*

The uncertainties of the capacitance estimation of the unaged samples, denoted δC, are presented in Fig. 4. For most of the cases, it occurs that $\delta C/C \cong 0.5\%$.

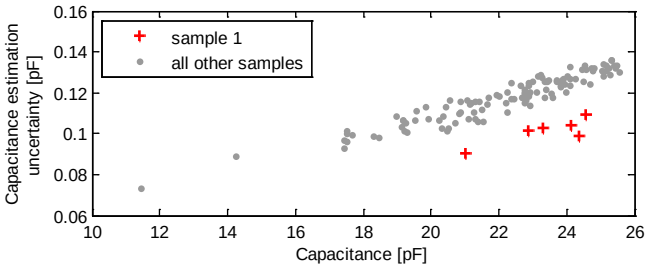

Fig. 4. Uncertainty of capacitance estimation vs. capacitance estimate

Interestingly, estimation uncertainty of all points on a single sample (sample 1 in Fig. 5) is slightly lower than the one of other samples.

IV. Analysis of Unaged Insulation

In this section the consistency of the insulation manufacturing quality is analysed. It is expected that the impedance measurements taken from each sample (note that the impedance has been measured as 6 equally spaced points at each sample) are characterised by comparable mean and standard deviation values. For visual inspection purpose measurements of capacitance and resistance of all new samples are presented in Fig. 5 and Fig 6, respectively. As the capacitance estimate is significantly less affected by measurement noise inaccuracies than the resistance estimate, the capacitance estimates have been used to assess the consistency of the manufacturing quality.

Firstly, the variance of the capacitance measurements taken for each sample has been considered. For every sample the mean value and standard deviation, denoted as μ_i and σ_i, respectively, of the six measured capacitance values have been calculated (the subscript i denotes the sample number). These are presented in Table I.

TABLE I
MEAN VALUE (μ_i) AND STANDARD DEVIATION (σ_i) OF 6 ESTIMATED CAPACITANCE VALUES (IN PICOFARADS) FOR EVERY SAMPLE

i	**1**	**2**	**3**	**4**	**5**	**6**	**7**
σ_i	1.3	1.3	1.5	4.5	3.5	1.6	2.1
μ_i	23.3	22.1	21.7	19.3	20.5	23.3	22.7
i	**8**	**9**	**10**	**11**	**12**	**13**	**14**
σ_i	2.4	2.8	2.1	1.7	2.2	2.1	1.9
μ_i	21.6	22.0	22.1	22.7	23.2	22.8	20.1
i	**15**	**16**	**17**	**18**	**19**	**20**	
σ_i	2.0	2.7	1.2	2.7	1.9	2.6	
μ_i	23.9	21.0	23.9	21.9	23.1	21.9	

Subsequently, for every pair of samples, i and j, a hypothesis that $\sigma_i = \sigma_j$ has been tested with the probability level of 0.05, cf. [33]. (Also all further hypotheses have been tested with the probability level 0.05). This hypothesis has been rejected for some pairs (i, j), namely (1,4), (2,4), (3,4), (4,6), (4,11), (4,17), and (5,17). In order to eliminate number of potential false positives, Benjamini and Hochberg (BH) correction has been applied. Multiple hypothesis that all pairs (4, i), $i = 1, \dots, 3, 5, \dots 20$, have equal variances has been carried out applying BH correction with false discovery rate of 0.05. Subsequently the test has been repeated for all pairs (17, i) , $i = 1, \dots 16, 18, \dots, 20$. The hypothesis has not been rejected for any of the pairs, hence it can be concluded that all samples have equal variance of capacitance values.

Then the procedure has been repeated to assess whether all samples are characterise with equal mean value. The multiple hypothesis that pairs (14,i), $i = 1, \dots 13, 15, \dots, 20$ have equal mean with application of the BH correction indicated that samples 14 and 17 have distinct mean value. However, considering that false discovery rate is $\delta = 0.05$ it is expected that in 5 % of the cases the hypothesis may be erroneously rejected[1]. Consequently, it is concluded that the capacitance of new samples can be characterised by a single

[1] The p-value is in the equal mean test (t-test) of samples 14 and 17 is 0.002 which is close to $\delta \frac{1}{19} = 0.0026$.

distribution with mean values of 22.17 and standard deviation of 2.46.

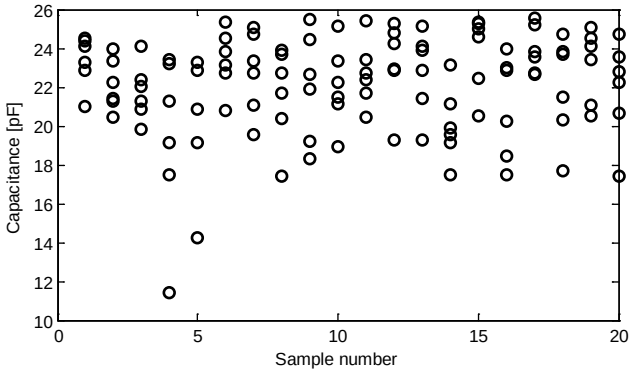

Fig. 5. Comparison of capacitance values measured at each sample.

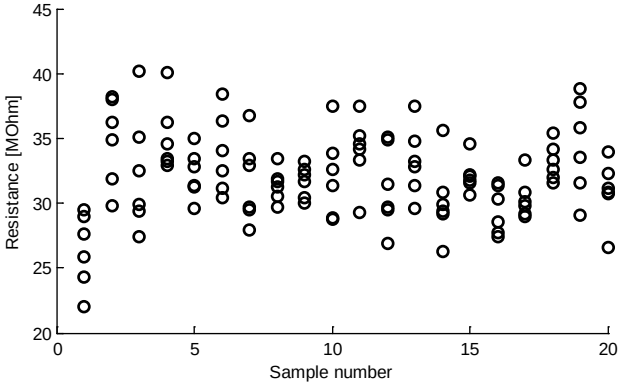

Fig. 6. Comparison of resistance values measured at each sample.

V. AGED INSULATION

We observed previously [31] that the capacitance of the majority of aged insulation samples is lower than 20 pF regardless of the length of ageing time. The only exceptions from this rule were insulation samples aged at 230 °C, where the capacitance drops from 22-24 pF to around 14 pF between 200 and 800 hours of ageing. Based on these observations a preliminary conclusion is made that the reduction of capacitance to $C < C_d \approx 20$ pF is an indicator of a thermal degradation, which is, however, not an end-of-life condition. (Note that for 18 % of new insulation samples $C < 20$ pF, thus the absolute capacitance cannot be a sole indicator of degradation). Furthermore, the degradation mechanism seems to be dependent on the temperature at which the material is aged, which is indicated by different capacitance of samples aged at 230 °C.

As the most pronounced variations in the electrical properties of insulation were observed in the case of ageing at 230 °C, these results are presented first in Subsection A. Subsections B and C analyse both the resistance and capacitance of the insulation aged at the other temperatures.

A. *Thermal ageing of insulation at 230 °C*

Fig. 7 presents insulation capacitance as function of time spent at 230 °C, denoted *t*. Mean values and standard deviations of the insulation capacitance for different values of *t* are presented in Table II.

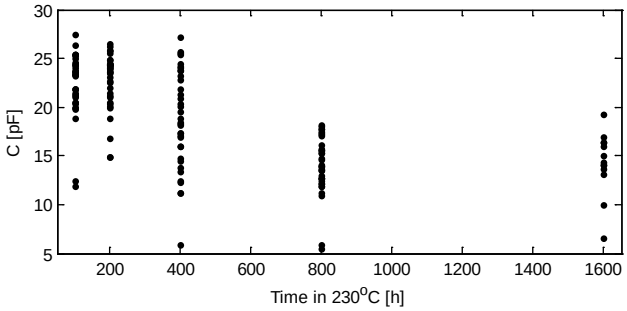

Fig. 7. Capacitance as function of time for insulation aged in 230 °C.

TABLE II
MEAN AND STANDARD DEVIATION OF CAPACITANCE.

Time, *t* [h]	100	200	400	800	1600
Mean [pF]	22.4±1.1	22.7±1.0	18.9±1.7	14.2±1.0	14.3±1.8
Standard deviation [pF]	3.3 (2.2-4.8)	2.9 (1.9-4.3)	5.0 (3.3-7.4)	3.0 (2.0-4.4)	3.2 (1.7-6.6)

The capacitance appears to decrease with time. However, this relationship is nonlinear. Also, note that the capacitance of the unaged insulation is 24.0 ± 0.6 pF, which is close to the capacitance of insulation aged at 230 °C for $t \leq 200$. We therefore hypothesise that a certain degradation phenomenon occurred between 200 and 800 hours leading to the capacitance drop from around 22-24 pF to around 14 pF (note that occurrence of this mechanism is not an end-of-life condition).

Fig. 8 compares histograms of capacitance measurements for ageing times greater and lower than 400 hours, i.e. before and after the aforementioned ageing phenomenon occurred. It is observed that the distribution of capacitance for $t < 400$ is negatively skewed. However, bearing in mind results from Section IV, it is assumed in the further analysis that the relatively low capacitance values obtained for $t < 400$ are due to manufacturing differences rather than thermal ageing. Distributions of capacitance values for $t < 400$ and $t > 400$ have been approximated with normal distributions $\mathcal{N}(23.1, 4.8)$[2] and $\mathcal{N}(14.2, 9.1)$, respectively, where $\mathcal{N}(\mu, \sigma^2)$ denotes normal distribution with mean μ and variance σ^2. These are presented in Fig. 9.

Subsequently, a decision boundary $C_d = 19.1$ pF has been calculated for which the capacitance probability density functions for the two considered cases ($t < 400$ h and $t > 400$ h) are equal. Thus, it is further assumed that the decrease of

[2] In the case of $t < 400$, 4 measurements with capacitances lower than 15 pF have been excluded from the estimation.

the capacitance below 19.1 pF indicates that the aforementioned degradation phenomenon has occurred.

Fig. 10 presents the insulation resistance as function of time of ageing at 230 °C. It is observed that for the first 400 hours the resistance decreases. (Note that the uncertainty of the resistance estimation increases with R, and that the four outliers visible in Fig. 10 for $t = 200$ h, for which the estimated resistance is greater than 44 MΩ, have estimation uncertainty of 11.7 MΩ on average, whilst the average estimation uncertainty for the remaining measurements for $t = 200$ h is 6.7 MΩ.) Subsequently, after 400 hours of ageing the resistance reaches its minimum (the average resistance estimation uncertainty for $t = 200$ h is 2.1MΩ), then the resistance increases.

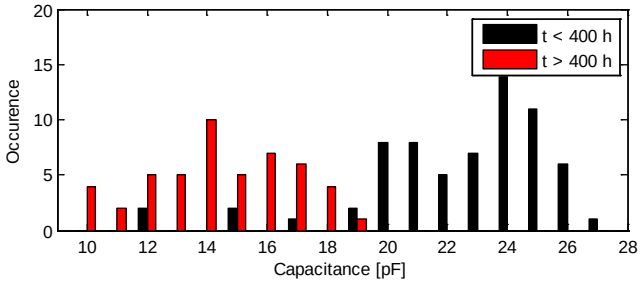

Fig. 8. Comparison of capacitance histograms for ageing time greater and lower than 400 hours

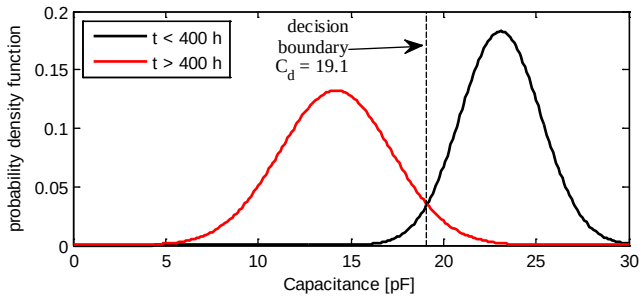

Fig. 9. Gaussian approximation of capacitance distributions for ageing time greater and lower than 400 hours.

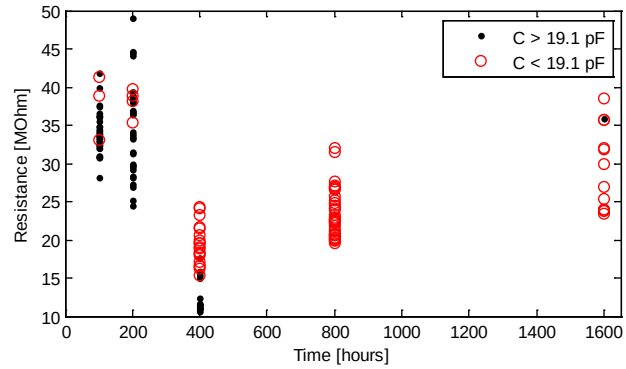

Fig. 10. Insulation resistance as function of time of ageing at 230 °C. Measurements for which capacitance exceeds 19.1 pF are denoted with red dots, whilst points for which $C < C_d$ are denoted with black circles

Furthermore, after 400 hours of ageing there is a clear separation between the resistance of 17 points with $C > C_d$ and 19 points for which $C < C_d$, see Fig. 10. This is also visible in Fig. 11, where measured capacitance has been plotted against resistance for $t = 400$ hours.

The differences between the electrical properties of different points measured at a single insulation sample aged at 230 °C for $t = 400$ are much smaller than the differences between measurements taken at different samples, see Fig. 11. This could be due to the differences between insulation samples due to manufacturing quality. Therefore, it is expected that the whole area of an insulation sample ages at approximately the same rate, whereas degradation rates may differ amongst insulation samples. It is observed that the capacitance measured at samples 1, 2 and 3 aged for 400 hours is greater than C_d (except for a single point in sample 3 which has capacitance of 18.4 pF which is close to 19.1 pF), whilst the capacitance of samples 4, 5 and 6 is lower than C_d.

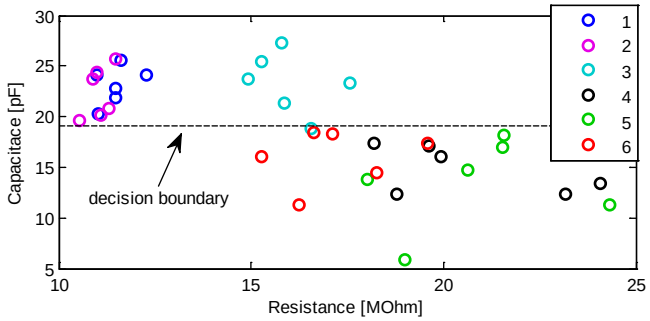

Fig. 11. Resistance and capacitance of insulation aged for 400 hours at 230 °C. Different colours denote measurements taken from different samples

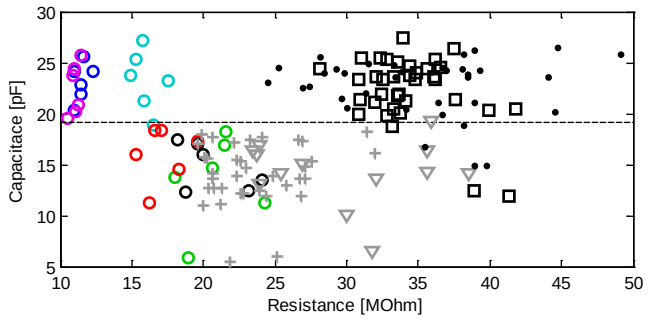

Fig. 12. Electrical properties of insulation with respect to ageing time at 230 °C. Black squares – $t = 100$ h, black dots – $t = 200$ h, grey crosses – $t = 800$ h, grey triangles – $t = 1600$ h, coloured circles – $t = 400$ h (cf. Fig. 11).

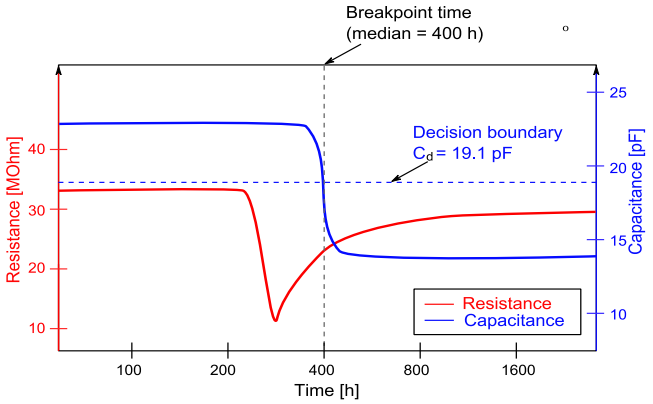

Fig. 13. Schematic representation of electrical properties of insulation samples aged at 230 °C.

Fig. 12 compares the resistance and the capacitance of insulation for t = 400 with the electrical properties of the insulation aged for times less than and more than 400 hours. Comparing Fig. 11 and Fig. 12 the following degradation mechanism is observed: for the first 200 hours of ageing at 230 °C no significant change of electrical properties of insulation are noted; the expected values of resistance and capacitance of insulation are ≈ 35 MΩ and ≈ 23 pF, respectively. Then the resistance drops to $R_{min} \approx 11$ MΩ. Following the rapid reduction of resistance the capacitance drops to expected values of ≈ 14 pF, whilst the resistance slowly increases. This process has been summarised in Fig. 13 where changes of both resistance and capacitance are plotted against time.

In this regard, it can be assumed that amongst the six samples aged for 400 hours (Fig. 11 and 12), degradation of sample 3 is the least advanced; samples 1 and 2 are at a similar stage of ageing and their capacitance is likely to reduce, whilst degradation of sample 5 is most advanced.

Note that the exact mechanism of ageing is not known at this stage, and further examination of the chemical properties of the aged insulation material is required to validate the above empirical results. Additionally, the resistance and capacitance values in the above degradation results are provisional and approximate. For example, since measurements are taken every several hundred hours it is not known whether $R_{min} \approx 11$ MΩ is the minimum resistance throughout the degradation period.

B. Thermal ageing of insulation at T < 230 °C

In this subsection thermal ageing of insulation at T = 200 °C and T = 215 °C is considered. It is observed that the insulation capacitance does not depend on the time of ageing (mean value of 14.5 pF and standard deviation of 2.7 pF). Thus, it is concluded than during the first 100 hours of ageing the capacitance has dropped from approximately 22 pF to around 14 pF. Analogously to the procedure presented in Fig. 8 and 9, distribution of the capacitance of unaged samples has been compared with the capacitance distribution of insulation aged in T < 230 °C and the decision boundary C_d = 18.8 pF has been obtained[3].

On the contrary, the resistance varies with time. The resistance of the insulation aged at 215 °C firstly drops and then increases (see Fig. 14). A similar observation has been made with respect to ageing at 230 °C; however, without chemical analysis of the aged samples, it is not known whether these similar observations are due to the same phenomenon. Furthermore, the fact that the capacitance behaves differently at 230 °C suggests that these might be different phenomena.

Note that in the case of insulation aged at 200 °C for 400 hours (Fig. 14) there is a significant spread of resistance. Fig. 15 compares resistance values measured at different samples (aged at 200 °C for 400 hours). It is observed that the relatively large spread of resistance values is due to sample 6 in Fig. 15, whose resistance measurements were all relatively low. This might be an outlier, or sample 6 is at a different stage of the ageing process than samples 1-5. Comparing Fig. 10 and 14 we can draw a hypothesis that the ageing process at 200 °C is slightly slower than ageing at 230 °C. It appears that the 'dip' of the material resistance visible in Fig. 10 after 400 h of ageing in 230 °C happened in the case of sample 6 in Fig 15 (i.e. the six lowest resistance measurements for 400 h in Fig 14), and is yet to happen for the rest of the samples aged in 200 °C for 400 h.

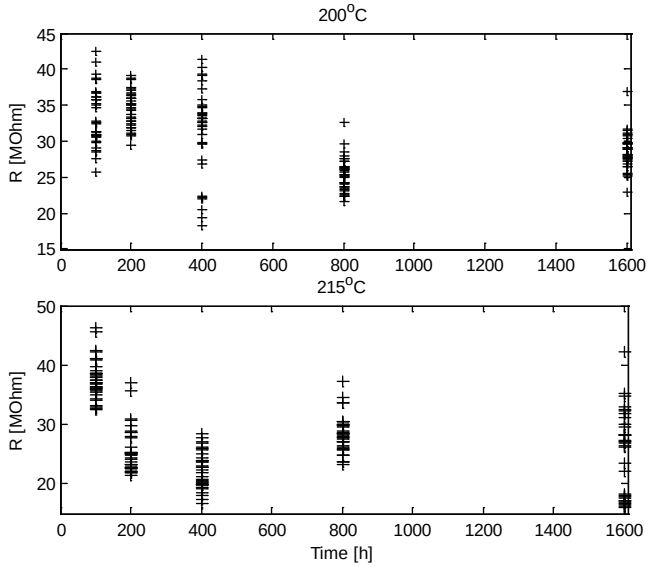

Fig. 14. Resistance of insulation aged in 200 °C and 215 °C as functions of time.

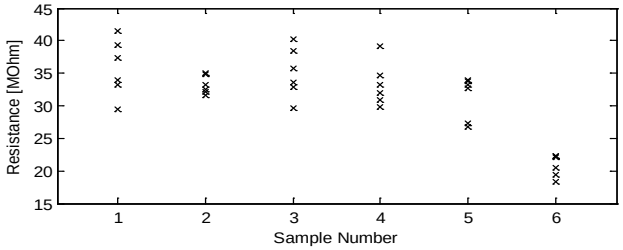

Fig. 15. Resistance of different insulation samples aged at 200 °C for 400 hours.

C. Thermal ageing of insulation at T > 230 °C

The resistance of insulation aged at higher temperatures than 230 °C exhibits different behaviour compared to the previous cases (see Fig. 16). Firstly, all insulation samples were catastrophically destroyed after 1600 hours at 245 °C and 260 °C, and 800 hours at 275 °C. It has also been observed that during ageing at high temperatures, the insulation delaminates, which leads to increased resistance readings, see Fig. 16. (Note that the resistance reading of a

[3] Samples 4 and 5 (see Fig. 5) has been excluded from this calculation.

delaminated sample corresponds to the combined resistance of insulation material and the air gap between the material and the electrode. Thus it is not representative of the material itself.) Reduction of resistance after 800 hours at 260 °C is probably due to fact that the insulation was partially burned, hence it becomes thinner.

Similarly to the low temperature case, the capacitance does not vary with ageing time (for T = 245, 260 °C the mean value and standard deviation are 14.8 and 2.8, respectively. In the case of ageing at 275 °C the capacitance is slightly elevated (mean value: 17.3, standard deviation 2.7), yet it does not depend on the ageing time.

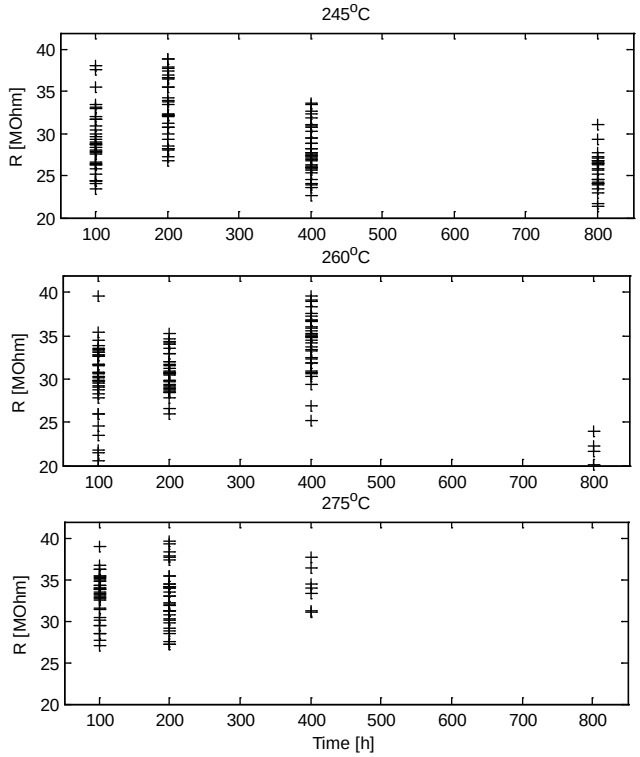

Fig. 16. Resistance of insulation aged at 245 °C, 260 °C and 275 °C as functions of time.

VI. Breakdown Voltage Characteristics

An important aspect of prognosis area is to relate the physical properties of a component to the remaining useful life. In this work's case, the remaining useful life is strongly related to the breakdown voltage of the thin film insulation material. This is because when the thin film insulating capabilities decrease there will be a developing current penetrating the thin film and leading eventually to inter-turn short circuits.

The early breakdown voltage (EBV) was measured using the conductive tape approach as defined in the standard CEI EN 60851-5. To make these measurements a CA6555 Chauvin-Arnoux 15kV Megohmmeter was used. The sample was placed in a dielectric case and four conducting aluminium tapes are attached to its surface (Fig. 17-a). The case is then closed (Fig. 17-b) so that there are no leakage currents/discharges between the electrodes and/or the sample.

Then the two high voltage electrodes are connected to the sample. One is connected at the end side of the copper bar inside the insulation, whereas the second is connected to one aluminum tape at a time (Fig. 17-c). The full setup is shown in Fig. 17-d. An optic cable was used to connect the Megohmmeter with a PC controlling the experiment and collecting the data, for safety reasons.

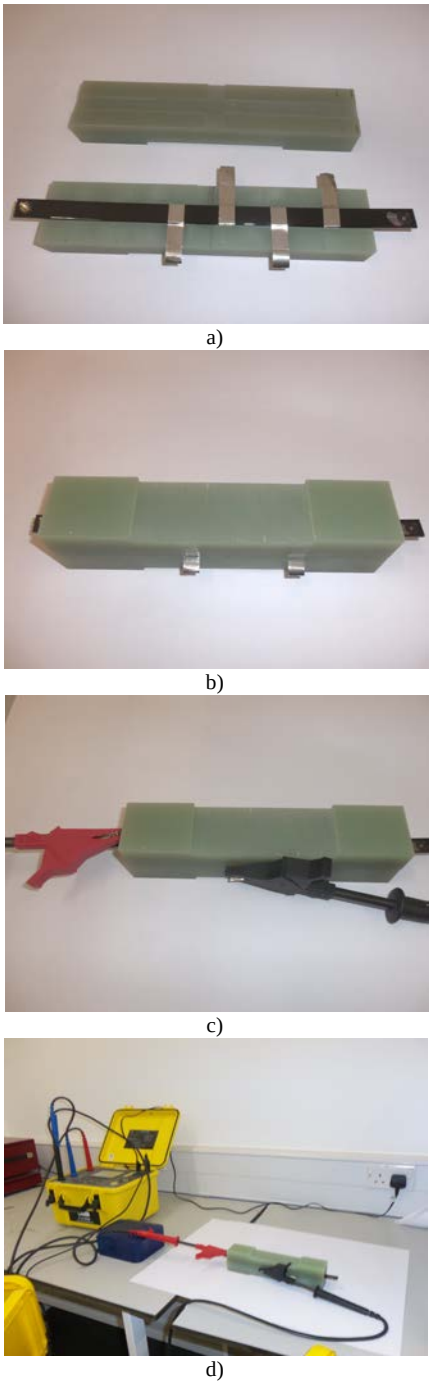

Fig. 17. Preparation of the samples for the breakdown voltage testing: a) attaching the aluminium tape strips, b) shielding the sample, c) connecting the high voltage electrodes and d) full setup.

When the connections are ready, the Megohmmeter is set to produce voltage ramps starting at 500V and ending at 15kV. The duration of the ramp is 13 minutes. When the breakdown takes place, the applied high voltage is immediately shut down and its instantaneous value is monitored and stored.

A. Analysis of breakdown voltage measurements

Tables III and IV present, respectively, mean and standard deviations of breakdown voltage (BV) measurements of insulation samples aged at different combinations of temperatures and times. Additionally, Table V presents median values of BV for each combination of temperature and time. Mean values of BV measurements for considered combinations of temperature and time (and the 95 % confidence bounds of mean estimation) are presented in Fig. 18.

TABLE III
MEAN VALUES OF BREAKDOWN VOLTAGE [KV]; NUMBERS IN BRACKETS DENOTE CONFIDENCE BOUNDS (CALCULATED USING STANDARD T-TEST)

		Temperature [ºC]			
		200	215	230	All temperatures
Time [h]	100	7.56 (7.14-7.94)	8.15 (7.44-8.86)	7.76 (7.12-8.40)	7.90 (7.55- 8.25)
	200	7.27 (6.87-7.68)	6.82 (6.27-7.38)	6.98 (6.59-7.37)	7.29 (7.01-7.57)
	400	7.08 (6.74-7.41)	6.83 (6.56-7.10)	7.38 (6.73-8.03)	7.30 (7.05-7.55)
	800	7.05 (6.69-7.42)	6.36 (6.13-6.59)	6.70 (6.29-7.11)	6.68 (6.51-6.86)
	1600	6.47 (6.27-6.67)	6.48 (6.15-6.82)	6.72 (6.17-7.28)	6.53 (6.35-6.71)
	All times	7.11 (6.95-7.27)	6.99 (6.74-7.24)	7.16 (6.92-7.41)	
new samples		8.96 (7.94-9.98)			

TABLE IV
STANDARD DEVIATION OF BREAKDOWN VOLTAGE [KV]]; NUMBERS IN BRACKETS DENOTE CONFIDENCE BOUNDS (CALCULATED USING F-TEST)

		Temperature [ºC]			
		200	215	230	All temperatures
Time [h]	100	0.94 (0.73-1.32)	1.98 (1.54-2.77)	1.45 (1.13-2.03)	1.72 (1.51-2.01)
	200	0.93 (0.72-1.31)	1.30 (1.01-1.83)	0.90 (0.70-1.26)	1.37 (1.20-1.60)
	400	0.77 (0.60-1.09)	0.63 (0.49-0.89)	1.52 (1.18-2.15)	1.23 (1.08-1.44)
	800	0.80 (0.62-1.15)	0.54 (0.42-0.75)	0.97 (0.75-1.35)	0.82 (0.72-0.97)
	1600	0.43 (0.33-0.61)	0.83 (0.65-1.17)	0.78 (0.53-1.42)	0.68 (0.57-0.83)
	All times	0.86 (0.76-0.98)	1.39 (1.23-1.59)	1.25 (1.10-1.44)	
new samples		3.47 (2.88-4.36)			

TABLE V
MEDIAN VALUES OF BREAKDOWN VOLTAGE [KV]

		Temperature [oC]			
		200	215	230	245
time [h]	100	7.59	7.71	7.12	7.69
	200	7.07	6.58	6.80	7.29
	400	6.99	6.65	6.84	7.13
	800	6.73	6.27	6.60	6.42
	1600	6.47	6.30	6.92	
new samples		9.26			

A strong dependency between the ageing temperature and breakdown voltage has been observed. However, no statistically significant difference has been observed between insulation samples aged for the same time at different temperatures. Furthermore, it is observed that the standard deviation of BV of new (unaged) samples is significantly greater than the standard deviation measured in aged insulation samples. The standard deviation of BV measurements also appears to reduce as with an increase of ageing time. Fig. 19 compares histograms of BV measurements of new samples with histograms of BV measurements of samples aged for 100 h and 1600 h in 200 ºC. This result indicates that the significant spread of results for unaged samples is rather due to the material properties than the measurement method. Note that four BV measurements at four different points have been taken at each sample. However, the four outliers visible in Fig 19 (i.e. BV measurement taken at unaged samples which are lower than 3 kV), have been measured at four different samples.

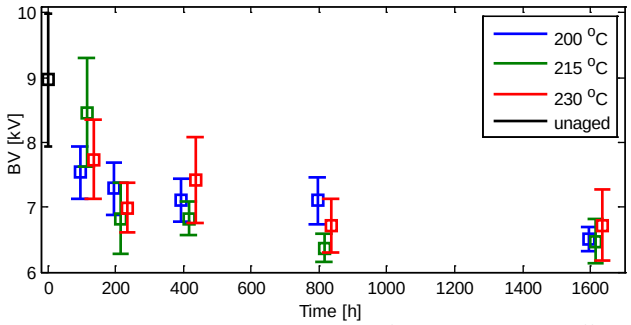

Fig. 18. Breakdown voltage measurements of insulation aged at different temperatures and times.

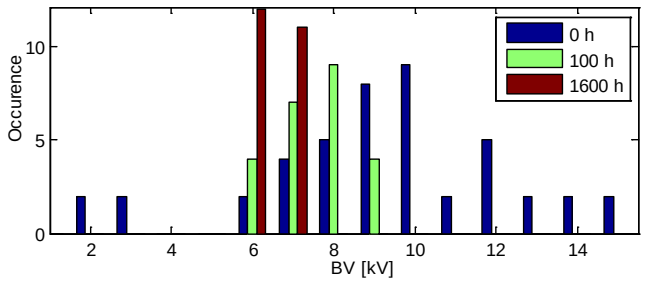

Fig. 19. Histograms of BV measurements of samples aged at 200 ºC (for 100 and 1600 hours) compared to histogram of BV measurements of unaged samples.

The breakdown voltage has been modelled as a function of time using the following logarithmic relationship:

$$BV = a - b\log_{10}(t-1) \qquad (2)$$

where BV [kV] denotes breakdown voltage, t [h] denotes time, and terms a and b are model parameters. Since distribution of BV measurements is not Gaussian and there are outliers in the data, parameters have been estimated using median regression which is more robust to outliers as opposed to mean regression (i.e. the least squares method). Parameters of model (2) have been estimated for three different values of ageing temperature (i.e. 200, 215, and 230 °C). Additionally, a fourth model which fits all the data (all temperatures) has been calculated. Parameters of the four cases of model (2) and their 95 % confidence bounds (see [32] for more details) are presented in Table VI.

Modelled median values of BV for different temperatures are plotted in Fig. 20. The 95 % confidence bounds of each model[4] have also been plotted. Although the differences in the BV models for different temperatures are not statistically significant (see large confidence bounds), the nominal models show that the ageing in 200 °C (solid blue line in Fig. 20) progresses more slowly than ageing at higher temperatures (i.e. 215 and 230 °C), which corresponds to the time evolution of material resistance in observed in Fig. 10 and 14 (see Section V B.).

TABLE VI
PARAMETERS OF BV MODEL (2) AND THEIR CONFIDENCE BOUNDS

Temperature [oC]	a	b
200	9.262 ± 0.549	0.873 ± 0.247
215	9.262 ± 0.589	0.959 ± 0.247
230	9.218 ± 0.607	0.951 ± 0.286
all data	9.262 ± 0.421	0.896 ± 0.172

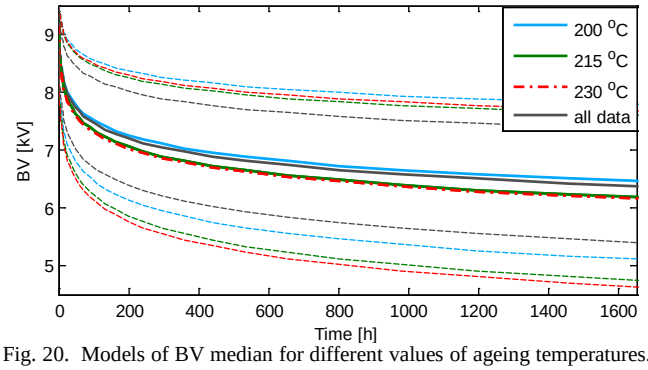

Fig. 20. Models of BV median for different values of ageing temperatures. Dashed lines of respective colours denote confidence bounds of the models.

VII. CONCLUSIONS AND FURTHER WORK

Impact of ageing temperature and time on the electrical properties of the PAI insulation was analysed. It is observed that during ageing at temperatures lower than or equal to 230 °C, the insulation resistance exhibits a particular trend: it decreases at first, followed by an increase after approximately 400 hours. It also appears that this trend in material resistance is slightly slower for samples aged in 200 °C than for material aged in 215 °C and 230 °C. Additionally, breakdown voltage measurements lead to similar conclusion – material ageing appears to progress more slowly in 200 °C.

On the contrary, while ageing at temperatures of 245 °C and higher, the insulation resistance rather increases, which may be an effect of delamination [31].

Furthermore, for almost all aged samples the capacitance of the equivalent circuit model is lower than 20 pF, whilst the average capacitance of new samples is 22 pF.

Moreover, the study of new (unaged) insulation samples has been carried out for comparison purposes. The capacitance of new samples can be characterised by a single distribution with mean value of 22.17 and standard deviation of 2.46. The mean and median of breakdown voltage (BV) of new samples is significantly higher than the one of aged material, which is an expected result. Interestingly, the standard deviation of BV measurements of new insulation is significantly higher than the standard deviation of BV measurements of aged samples.

[4] Confidence bounds of median BV models plotted in Fig. 20 represent the most extreme cases of the parameters in Table VI.

REFERENCES

[1] J. Tavner, "Review of condition monitoring of rotating electrical machines," *IET Elec. Pow. Appl.*, Vol. 2, No. 4, pp. 215-247, 2008.

[2] H. O. Seinsch, "Monitoring und Diagnose elektrischer Maschinen und Antriebe," in Proc. VDE Workshop, Allianz Schadensstattistik an HS Motoren, 1996-1999, 2001.

[3] P. Zhang, Y. Du, T. G. Habetler, and B. Lu, "A survey of condition monitoring and protection methods for medium-voltage induction motors," *IEEE Trans. Ind. Appl.*, vol. 47, no. 1, pp. 34–46, Jan./Feb. 2011.

[4] "Report of large motor reliability survey of industrial and commercial installations, Part I," *IEEE Trans. Ind. Appl.*, Vol. IA-21, No. 4, Jul./Aug. 1985, pp. 853-864.

[5] "Report of large motor reliability survey of industrial and commercial installations, Part II," *IEEE Trans. Ind. Appl.*, Vol. IA-21, No. 4, Jul./Aug. 1985, pp. 865-872.

[6] "Report of large motor reliability survey of industrial and commercial installations, Part III," *IEEE Trans. Ind. Appl.*, Vol. IA-23, No. 1, Jan./Feb. 1985, pp. 153-158.

[7] R. M. Tallam, S. B. Lee, G. C. Stone, G. B. Kliman, J. Y. Yoo, T. G. Habetler, R. G. Harley "A survey of methods for detection of stator-related faults in induction machines," IEEE Trans. Ind. Appl., Vol. 43, No. 4, pp. 920-933, Jul./Aug. 2007.

[8] A. Bellini, F. Filippetti, C. Tassoni and G. A. Capolino, "Advances in diagnostic techniques for induction machines," IEEE Trans. Ind. Elec., Vol. 55, No. 12, pp. 4109-4126, Dec. 2008.

[9] G. M. Joksimovic and J. Penman, "The detection of inter-turn short circuits in the stator windings of operating motors," IEEE Trans. Ind. Elec., Vol. 47, No. 5, pp. 1078-1084, Oct. 2000.

[10] K. N. Gyftakis and J. C. Kappatou, "The zero-sequence current as a generalized diagnostic mean in Δ-connected three-phase induction motors," IEEE Trans. Ener. Conv., Vol. 29, No. 1, pp. 138-148, Mar. 2014.

[11] C. Gerada, K. Bradley, M. Sumner, P. Wheeler, S. Pickering, J. Clare, C. Whitney and G. Towers, "The results do mesh," IEEE Ind. Appl. Mag., Vol. 13, No. 2, pp. 62-72, Mar/Apr. 2007.

[12] S. Williamson and K. Mirzoian, “Analysis of cage induction motors with stator winding faults,” IEEE Trans. Power App. Syst., vol. PAS-104, no. 7, pp. 1838–1842, Jul. 1985.
[13] A. J. M. Cardoso, S. M. A. Cruz, and D. S. B. Fonseca, “Inter-turn stator winding fault diagnosis in three-phase induction motors, by Park’s vector approach,” IEEE Trans. Ener. Conv., vol. 14, no. 3, pp. 595–598, Sep. 1999.
[14] J. F. Martins, V. F. Pires, and A. J. Pires, “Unsupervised neural-network-based algorithm for an on-line diagnosis of three-phase induction motor stator fault,” IEEE Trans. Ind. Electr., vol. 54, no. 1, pp. 259–264, Feb. 2007.
[15] S. M. A. Cruz and A. J. M. Cardoso, “Stator winding fault diagnosis in three-phase synchronous and asynchronous motors, by the extended Park’s vector approach,” IEEE Trans. Ind. Appl., vol. 37, no. 5, pp. 1227–1233, Sep./Oct. 2001.
[16] A. M. da Silva, R. J. Povinelli, and N. A. O. Demerdash, “Induction machine broken bar and stator short-circuit fault diagnostics based on three-phase stator current envelopes,” IEEE Trans. Ind. Electr., vol. 55, no. 3, pp. 1310–1318, Mar. 2008.
[17] M. Drif and A. J. M. Cardoso, "Stator Fault Diagnostics in Squirrel Cage Three-Phase Induction Motor Drives Using the Instantaneous Active and Reactive Power Signature Analyses," *IEEE Trans. Ind. Inf.*, Vol. 10, No. 2, pp. 1348-1360, May 2014.
[18] A. S. Babel and E. G. Strangas, “Condition-Based Monitoring and Prognostic Health Management of Electric Machine Stator Winding Insulation”, IEEE ICEM, pp. 1855-1861, Berlin, Germany, Sep. 2014.
[19] G. C. Stone, E. A. Boulter, I. Culbert and H. Dhirani, “Electrical Insulation for Rotating Machines-Design, Evaluation, Aging, Testing and Repair”, IEEE Press Series on Power Engineering, 2004.
[20] A. J. Gonzalez, M. S. Baldwin, J. Stein and N. E. Nilsson, “Monitoring and Diagnosis of Turbine-driven Generators,” Prentice Hall, 1995.
[21] I. Culbert, H. Dhirani and G. C. Stone, “Handbook to Assess the Insulation Condition of Large Rotating Machines,” EPRI Power Plant Electrical Reference Series, Vol. 16, 1989.
[22] K. Younsi, P. Neti, M. Shah, J. Y. Zhou, J. Krahn, and K. Weeber, “On-line Capacitance and Dissipation Factor Monitoring of AC Stator Insulation,” *IEEE Trans. Diel. Elec. Ins.*, Vol. 17, No. 5, pp. 1441-1452, Oct. 2010.
[23] M. Farahani, E. Gockenbach, H. Borsi, K. Schäfer, and M. Kaufhold, “Behavior of Machine Insulation Systems Subjected to Accelerated Thermal Aging Test,” *IEEE Trans. Diel. Elec. Ins.*, Vol. 17, No. 5, pp. 1364-1372, Oct. 2010.
[24] N. Lahoud, J. Faucher, D. Malec and P. Maussion, “Electrical Aging of the Insulation of Low-Voltage Machines: Model Definition and Test With the Design of Experiments,” *IEEE Trans. Ind. Elec.*, Vol. 60, No. 9, pp. 4147-4155, Sep. 2013.
[25] S. Savin, S. Ait-Amar and D. Rogers, “Cable Aging Influence on Motor Diagnostic System,” *IEEE Trans. Diel. Elec. Ins.*, Vol. 20, No. 4, pp. 1340-1346, Aug. 2013.
[26] F. Salameh, A. Picot, M. Chabert, E. Leconte, A. Ruiz-Gazen and P. Maussion, “Variable Importance Assessment in Lifespan Models of Insulation Materials: A Comparative Study”, IEEE SDEMPED, pp. 198-204, Guarda, Portugal, Sep. 2015.
[27] C. Zoeller, M.A. Vogelsberger, R. Fasching, W. Grubelnik and Th.M. Wolbank, “Evaluation and Current-Response Based Identification of Insulation Degradation for High Utilized Electrical Machines in Railway Application”, IEEE SDEMPED, pp. 266-272, Guarda, Portugal, Sep. 2015.
[28] S. Thomas, K. Joseph, S. K. Malhotra, K. Goda and M. S. Sreekala, “Polymer Composites Volume 1: Macro- and Mircocomposites” WILEY-VCH, 2012.
[29] A. Hulme and J. Cooper, “Life prediction of polymers for industry,” *Elsevier Sealing Technology*, Vol. 2012, No. 9, pp. 8-12, Sep. 2012.
[30] R. Morin and R. Bartnikas, “Multistress Aging of Stator Bars in a Three-Phase Model Stator Under Load Cycling Conditions,” *IEEE Trans. Ener. Conv.*, Vol. 27, No. 2, pp. 374-381, Jun. 2012.
[31] K. N. Gyftakis, M. Sumislawska, D. F. Kavanagh, D. Howey and M. McCulloch “Dielectric Characteristics of Electric Vehicle Traction Motor’s Winding Insulation under Thermal Ageing”, *IEEE Trans. Ind. Appl.*, early access.
[32] L. Ljung, *System Identification: Theory for the User*. Prentice Hall, 1999.
[33] M. H. DeGroot and M. J. Schervish, *Probability and Statistics*, 4th ed. Pearson Education, 2002.

Malgorzata Sumislawska received MSc. in Teleinformatics from Wroclaw University of Techlology, Wroclaw Poland (2009) and MSc. in Systems and Control from Coventry University (CU), Coventry, UK (2009). In 2012 she obtained PhD degree in Mathematics and Control Engineering from CU. She is currently a Lecturer in System Identification at CU. Her research includes fault detection and diagnosis, data-based reduced order modeling for control diagnostics and prognostics, state and parameter estimation, and filtering.
(Email – malgorzata.sumislawska@coventry.ac.uk)

Konstantinos N. Gyftakis (M’11**)** was born in Patras, Greece, in May 1984. He received the Diploma in Electrical and Computer Engineering from the University of Patras, Patras, Greece in 2010. He pursued a Ph.D in the same institution in the area of electrical machines condition monitoring and fault diagnosis (2010-2014). Then he worked as a Post-Doctoral Research Assistant in the Dept. of Engineering Science, University of Oxford, UK. He is currently a Lecturer, Faculty of Engineering, Environment and Computing, Coventry University, UK. His research activities are in fault diagnosis, condition monitoring and degradation of electrical machines. He has authored/co-authored more than 30 papers in international scientific journals and conferences. (E-mail: k.n.gyftakis@ieee.org).

Darren F. Kavanagh is an Asst. Lecturer at the Institute of Technology Carlow, Ireland. Prior to this he conducted postdoctoral research at the University of Oxford investigating the area of degradation and failure analysis of electric machines with specific applications in electric vehicles. Darren completed his Ph.D. research at Trinity College Dublin in 2011. His doctoral research was in the area of advanced signal processing and pattern recognition for acoustic signals. In 2006, he was awarded an EMBARK scholarship by the Irish Research Council to pursue a Ph.D. on the topic of acoustic signal processing. He was awarded the prestigious Minister’s Silver Medal for Science by the Minister for Education (Ireland) in 2004. He has gained valuable academic experience at educational institutions such as, the University of Oxford, Trinity College Dublin and the Institute of Technology Tallaght, ITT Dublin. He has also benefited greatly from industrial experience at Alcatel Lucent-Bell Laboratories, Intel, and Xilinx.

Malcolm D McCulloch. In 1993 Malcolm moved to Oxford University and to start up the Electrical Power Group (EPG), where is an Associate Professor. The group’s focus is to developing, and commercialise, sustainable energy technologies in the four sectors of energy for development, domestic energy use, transport and renewable generation. His work addresses transforming existing power network, designing new power network for the developing world, developing new technology for electric vehicles and developing approaches to integrated mobility. He has over 100 Journal and refereed conference papers, 15 patents and 4 spinout companies.

Keith J Burnham was a founding member of the Control Theory and Applications Centre in 1987, and a professor of industrial control systems since 1999. He received BSc, MSc and PhD degrees in 1981, 1984 and 1991, respectively. Research includes self-tuning and adaptive control for nonlinear industrial systems, with particular interest bilinear systems. Strong

collaboration involving consultancy with a wide range of industrial organisations, research with international academic organisations as well as an active involvement with the major UK professional bodies.

David A. Howey (M'10) received the B.A. and M.Eng. degrees from Cambridge University, Cambridge, U.K., in 2002 and the Ph.D. degree from Imperial College London, London, U.K., in 2010. He is currently an Associate Professor in the Energy and Power Group, Department of Engineering Science, University of Oxford, Oxford, U.K. He leads projects on fast electrochemical modeling, model-based battery management systems, battery thermal management, and motor degradation. His research interests include condition monitoring and management of electric and hybrid vehicle components.